A morphometric analysis of the forelimb in the genus Tapirus (Perissodactyla: Tapiridae) reveals influences of habitat, phylogeny and size through time and across geographical spac...

Article *in* Zoological Journal of the Linnean Society · October 2018

DOI: 10.1093/zoolinnean/zly019

CITATIONS
6

READS
1,179

4 authors:

Jamie Alexander MacLaren
University of Liège
36 PUBLICATIONS **40** CITATIONS
SEE PROFILE

Richard C. Hulbert
Florida Museum of Natural History
78 PUBLICATIONS **1,493** CITATIONS
SEE PROFILE

Steven C Wallace
East Tennessee State University
62 PUBLICATIONS **385** CITATIONS
SEE PROFILE

Sandra Nauwelaerts
University of Antwerp
86 PUBLICATIONS **858** CITATIONS
SEE PROFILE

Zoological Journal of the Linnean Society, 2018, **184**, 499–515. With 4 figures.

A morphometric analysis of the forelimb in the genus *Tapirus* (Perissodactyla: Tapiridae) reveals influences of habitat, phylogeny and size through time and across geographical space

JAMIE A. MACLAREN[1*], RICHARD C. HULBERT JR[2], STEVEN C. WALLACE[3] AND SANDRA NAUWELAERTS[1,4]

[1]*Department of Biology, Universiteit Antwerpen, Campus Drie Eiken, Universiteitsplein, Wilrijk, Antwerp, 2610, Belgium*
[2]*Florida Museum of Natural History, University of Florida, Dickinson Hall, Gainesville, Florida, FL 32611, USA*
[3]*Don Sundquist Center of Excellence in Paleontology, Department of Geosciences, East Tennessee State University, Johnson City TN 37614, USA*
[4]*Centre for Research and Conservation, Koninklijke Maatschappij voor Dierkunde (KMDA), Koningin Astridplein 26, Antwerp, 2018, Belgium*

Received 3 December 2017; revised 8 February 2018; accepted for publication 1 March 2018

The limb skeleton of tapirs (Perissodactyla: *Tapirus* spp.) was traditionally thought to exhibit morphological variation only as a result of changes in body size. Here, we test whether forelimb variation exhibited by *Tapirus* is solely an artefact of size fluctuations through the tapir fossil record or whether it is influenced by habitat differences. We investigated the forelimb osteology of 12 species of *Tapirus* using three-dimensional geometric morphometrics on laser surface scans. Aligned shape coordinates were regressed against intrinsic bone size to account for allometry. Taxa of equivalent body mass exhibited significant differences in size-corrected bone shape. Stable carbon isotope values were averaged per species as a proxy for habitat density. Multivariate regressions of the humerus, pisiform, cuneiform, unciform, third and fourth metacarpals revealed no significant influence of size on shape. The lateral carpals (pisiform, cuneiform, unciform) demonstrated variation across the habitat density gradient. Observed variation is likely driven by species in the extinct subgenus *Helicotapirus* tapirs, which inhabited drier, more open woodland than modern taxa. We conclude that tapir forelimb variation is not exclusively an artefact of body size, with lateral wrist bones displaying notable differences across a habitat density gradient, beyond that resulting from size and phylogenetic effects.

ADDITIONAL KEYWORDS: allometry – ecomorphology – geometric morphometrics – *Helicotapirus* – tapir.

INTRODUCTION

For many years the skeleton of the modern tapir *Tapirus* Brisson (Perissodactyla: Tapiridae) has been considered pleisiomorphic (Earle, 1893; Gregory, 1929; Simpson, 1945; Radinsky, 1965). The combination of a tetradactyl (four-toed) forelimb, unspecialized lophodont dentition and closed-habitat environments in which tapirs are currently found are analogous to the earliest ancestors of other modern perissodactyl groups, including rhinoceroses (Rhinocerotidae), equids (Equidae) and tapirs themselves (Holbrook, 2001; DeSantis & MacFadden, 2007; Secord, Wing & Chew, 2008; Bai *et al.*, 2017). Tapir postcranial anatomy has undergone little quantitative attention due to historical claims that tapir limb bones vary in shape only as an influence of changes in body size (Hershkovitz, 1954; Radinsky, 1965). Extant tapirs share several morphological features in common with Paleogene tapiroids (Radinsky, 1965; Holbrook, 1999;

*Corresponding author. E-mail: jamie.maclaren@uantwerpen.be

Colbert, 2005), with differences reported in the forelimb limited to the robusticity of the limb bones (associated with greater mass) and several features associated with greater cursoriality (e.g. loss of acromion of the scapula; Radinsky, 1965). This reported lack of variation in the tapir skeleton through time has in the past led authors to describe it as a 'living fossil' (Janis, 1984; Rustioni & Mazza, 2001), and to utilize tapir fossils as a robust indicator of forested habitats through time (DeSantis & MacFadden, 2007). However, recent quantitative examinations of forelimb osteology in modern *Tapirus* have revealed unexpected interspecific variation within this locomotor unit.

Quantitative investigations into extant tapir forelimb skeleton have recently revealed interspecific differences in keeping with different locomotor outcomes (MacLaren & Nauwelaerts, 2016, 2017). Most notably, variation was observed between tapirs sharing close phylogenetic affinity (*Tapirus pinchaque* and *T. terrestris*) but inhabiting different ecological biomes (Padilla & Dowler, 1994; Padilla, Dowler & Downer, 2010). Forelimb bone shape in *T. pinchaque*, a tropical yet high-altitude shrubland and cloud-forest species, was most divergent of all the modern taxa (MacLaren & Nauwelaerts, 2016, 2017; Ruiz-García *et al.*, 2016). Within these quantitative studies, differences were also found between taxa of greatly different body masses (e.g. *T. indicus* and *T. terrestris*), supporting the historical viewpoint on postcranial variation in tapirs (Earle, 1893; Hershkovitz, 1954; Radinsky, 1965). However, the range of body sizes within extant tapirs is not representative of the genus *Tapirus* as a whole, which includes at least 21 valid extinct species in addition to the four extant species and several subgenera (e.g. *Acrocodia*, *Helicotapirus* and *Megatapirus*). To truly test whether the morphology of the tapir postcranial skeleton is influenced solely by size, a greater range of taxa must be incorporated in a morphological analysis free of both isometric and allometric (size-dependent) shape variation.

In addition to studies revealing locomotor disparity within this apparently ecologically conserved clade (Hulbert, 2005; MacLaren & Nauwelaerts, 2016, 2017), ranges in habitat exploitation and dietary preferences have also been demonstrated in tapirs (DeSantis & MacFadden, 2007; Padilla *et al.*, 2010; DeSantis, 2011; Ruiz-García *et al.*, 2012) using stable carbon isotope ratios ($\delta^{13}C$) from tooth enamel (including: DeSantis & MacFadden, 2007; Secord *et al.*, 2008; Boardman & Secord, 2013). Disparity in stable isotope ranges has not been specifically linked to any morphological differences in either the cranial or postcranial skeleton of tapirs, despite evidence that tapirs in different time periods inhabited more open biomes compared to their current range of dense rainforest and *páramo* shrubland (MacFadden & Cerling, 1996; Koch, Hoppe & Webb, 1998; Kohn, McKay & Knight, 2005; Feranec & MacFadden, 2006; Hoppe & Koch, 2006; DeSantis & Wallace, 2008; DeSantis *et al.*, 2009, 2011; Padilla *et al.*, 2010; Perez-Crespo *et al.*, 2012; Nelson, 2014; Bocherens *et al.*, 2017). The functional and locomotor challenges of occupying a dense, closed-forest environment will differ to those of a more open habitat (Curran, 2015), and morphological differences may be expected between closed-canopy rainforest taxa and those existing in drier and more open woodland realms. Alternatively, the influence of phylogenetic relatedness may cause morphological conservancy within tapir limb bones, resulting in shape variability only with increasing body size (allometry).

Here, we investigate whether forelimb variation exhibited by a broad sample of *Tapirus* is simply an artefact of changes in size through the tapir fossil record (as suggested by previous authors: Simpson, 1945; Hershkovitz, 1954; Radinsky, 1965; Padilla & Dowler, 1994; Rustioni & Mazza, 2001) or whether differences in limb osteology are influenced by habitat variation. Based upon recent quantitative findings (Hulbert, 2005; MacLaren & Nauwelaerts, 2016, 2017), we use a three-dimensional geometric morphometric approach to test the hypothesis that habitat influences forelimb shape variation in tapirs after accounting for allometry (size-dependent shape). This approach is conducted on a series of extant and extinct *Tapirus* species across a spectrum of body sizes within a phylogenetic context.

INSTITUTIONAL ABBREVIATIONS

AMNH, American Museum of Natural History, New York; ETMNH, East Tennessee State University and General Shale Brick Museum of Natural History, Gray; FSL, Université Claude Bernard Lyon, Lyon; MEO, MuseOs Natuurhistorisch Museum, Koksijde; MNHN, Muséum National d'Histoire Naturelle, Paris; MVZ, Museum of Vertebrate Zoology, Berkeley; NHMW, Naturhistorisches Museum Wien, Vienna; RMNH, Naturalis Biodiversity Centre, Leiden; UF, Florida Museum of Natural History, Gainesville; UF/FGS, collection of the Florida Geological Survey, housed at the Florida Museum of Natural History; ZMB MAM, Museum für Naturkunde (Mammal Collections), Berlin.

METHODOLOGY

SPECIMENS

Forelimb material from extinct tapir species was laser scanned at the Florida Museum of Natural History (Gainesville, FL) and the Gray Fossil Site and General Shale Natural History Museum (Gray, TN). Species included *T. webbi* Hulbert, *T. polkensis* Olsen and the *Helicotapirus* species *T. lundeliusi* Hulbert, *T. haysii* Leidy and *T. veroensis* Sellards (Hulbert, 2010) (Table 1). These North American specimens were supplemented with scans from available postcranial elements of the

giant Asian tapir *Tapirus* (*Megatapirus*) *augustus* (American Museum of Natural History, NY) and the European tapirs *T. priscus* (Museum für Naturkunde, Berlin) and *T. arvernensis* (Université Claude Bernard Lyon). Individual limb elements were scanned with a FARO ScanArm Platinum V2 system with integrated FARO Laser Line Probe (≥50 μm resolution), and visualized using GEOMAGIC (GEOMAGIC QUALIFY v.10, Morrisville, NY, USA). Scans of fossil specimens were combined with previously analysed material representing the four extant tapir species (*T. terrestris* L., *T. pinchaque* Roulin, *T. bairdii* Gill and *T. indicus* Desmarest) (MacLaren & Nauwelaerts, 2016, 2017). Bones included the humerus, radius, pisiform, cuneiform, lunate, scaphoid, magnum, unciform and the second, third, fourth and fifth metacarpals. Extant specimens were collected from museums in Europe and the USA (see Table 1 in: MacLaren & Nauwelaerts, 2016); full details on specimens can be found in the Supporting Information (Appendix S1).

Geometric morphometrics

Landmark-based geometric morphometrics has been widely used for quantifying variation in shape between objects (e.g. Zelditch *et al.*, 2012; Klingenberg, 2016). A series of discrete points (landmarks), detailing biologically and operationally homologous features, were digitally placed on to each bone using LANDMARK EDITOR v.3.0 software (Wiley *et al.*, 2006). For full details on the three-dimensional landmark points selected, see MacLaren & Nauwelaerts (upper arm, 2016; autopodium, 2017). Raw landmark coordinates were exported to MORPHOJ v.1.06d (Klingenberg, 2011) and aligned using Generalized Procrustes Analysis (GPA) (Rohlf & Slice, 1990). GPA removes the effect of scale, location and orientation, aligning coordinate configurations based on a geometric centre (centroid). GPA produces an intrinsic size measure (centroid size; the sum of the squared distances from each landmark to the geometric centre), which was log-transformed and used for correcting shape data for allometric influence (Monteiro, 1999; Klingenberg, 2016). For full details regarding the choice of analysis to correct for allometric effects, see Supporting Information (Table S1).

Body mass estimation

To establish whether forelimb bone size could be used as a viable proxy for overall size, we estimated tapir body masses using linear regression equations based on humeral measurements described in Scott (1990); these were successfully applied to tapirs previously in Hulbert *et al.* (2009). Linear measurements for estimating body mass were chosen based on the highest squared correlation coefficients (R^2 ≥0.95) from ungulate regression equations (H3, H4 & H5; Scott, 1990; also see: Damuth & MacFadden, 1990, Supporting Information, Fig. S1). Linear measurements were performed on scanned humeri using the measuring tool in Geomagic Studio 10. Mass estimates for extant species were compared against published body mass brackets from live specimens (de Thoisy *et al.*, 2014). Body mass estimates from individual linear measurements were averaged, log-transformed and regressed against log-transformed centroid sizes ($_{log}$CS, from geometric morphometric analysis) to assess validity of using $_{log}$CS as a representative size measure. Full details on body mass estimations can be found in the Supporting Information (Fig. S1).

Regression, PCA and perMANOVA

Procrustes coordinates produced from GPA were regressed against log-transformed centroid size ($_{log}$CS) using multivariate regression (Monteiro, 1999; Zelditch *et al.*, 2012; Klingenberg, 2016), producing shape variables entirely independent of size effects (Klingenberg, 2016). Regression residuals were subsequently subjected to principal components analyses (PCAs). PCAs produced principal component scores of regression residuals (rPCs), with species' variation visualized in morphospace constructed in RStudio (RStudio Team, 2016). A permutational multivariate analysis of variance (perMANOVA) of regression residuals was used to test for interspecific differences (Anderson, 2001) in aligned coordinates. PerMANOVA was chosen because dependent variables exceeded sample (specimens) number, and group sizes did not vary greatly. PerMANOVA testing was performed in PAST v.3 (Hammer, Harper & Ryan, 2001), with pairwise perMANOVA testing (10 000 permutations) performed in RStudio using the 'RVAideMemoire' package (Hervé, 2016); *P*-values were corrected using false discovery rate protocol (Benjamini & Hochberg, 1995).

Ecological traits

Carbon isotope values ($\delta^{13}C$) from tooth enamel of tapir species were collated from published literature and averaged per species (Table 1; raw values in Supporting Information: Stable Carbon Isotopes). No isotope recordings were available for European tapir taxa. Average $\delta^{13}C$ recordings were assigned to one of four ranges, with each species falling within one range: >–13‰ (*T. haysii*, *T. lundeliusi*, *T. veroensis*); –13‰ to –14‰ (*T. webbi*, *T. polkensis*); –14‰ to –15‰ (*T. bairdii*, *T. pinchaque*); <–15‰ (*T. indicus*, *T. terrestris*). Significant differences between species mean $\delta^{13}C$ and species range $\delta^{13}C$ (habitat proxy) were tested for using one-way analysis of variance (ANOVA) in PAST v.3 (Hammer *et al.*, 2001) with Tukey's pairwise comparisons between *a priori* groups.

Table 1. Body mass estimates for *Tapirus* species based on humeral linear measurements; number of specimens (*N*), geographical origin (location), mean estimated BM ($\bar{x}$) in kg, standard deviation (SD), log-transformed body mass used in comparative analyses ($_{log}$BM), and average stable carbon isotope recording from literature ($\delta^{13}C$)

Species	*N*	location	$\bar{x}$	SD	$_{log}$BM	$\delta^{13}C$
T. (M.) augustus	1	SE Asia	631.4	-	6.45	-
T. priscus	1	Europe	349.8[a]	-	5.86	-
T. indicus	8	SE Asia	326.4	14.53	5.79	15.4
T. webbi	6	N America	293.3	31.59	5.68	13.0
T. sanyuanensis	1	SE Asia	284.0[b]	-	5.64	-
T. haysii	1	N America	279.2	-	5.63	12.2
T. veroensis	5	N America	232.1	18.46	5.45	12.7
T. bairdii	5	CS America	228.7	15.25	5.43	14.8
T. terrestris	5	S America	216.6	25.57	5.38	15.6
T. arvernensis	1	Europe	215.0[a]	-	5.37	-
T. lundeliusi	8	N America	202.8	23.62	5.31	12.8
T. pinchaque	4	S America	202.4	19.28	5.31	14.3
T. polkensis	6	N America	116.9	18.26	4.76	13.1

[a]Mass predicted from radius-humerus regression (see Supporting Information, Fig. S1).
[b]Measurements taken with permission from scaled images of humerus in Tong & Qiu (2008).

Informal tapir phylogeny

Tapirus has a deep-rooted evolutionary history (Holbrook, 1999; Norman & Ashley, 2000; Steiner & Ryder, 2011). To account for influence of phylogenetic relatedness on forelimb morphology, a composite phylogeny was assembled from published literary sources (Eisenmann & Guérin, 1992; Hulbert, 1995, 2005, 2010; Colbert, 2005; Tong, 2005; Steiner & Ryder, 2011; Holanda & Ferrero, 2013; Ruiz-García *et al.*, 2016). A phylogenetic tree was constructed in MESQUITE v.3.04, with branch lengths generated in RSTUDIO v.1.0.143 (RStudio Team, 2016) using the 'paleotree' package (Bapst, 2012). Branch lengths were calculated based on first/last occurrence dates compiled from the literature (Colbert & Hooijer, 1953; Guérin & Eisenmann, 1982; Eisenmann & Guérin, 1992; Hulbert, 1995, 2005, 2010; Czaplewski, Puckette & Russell, 2002; Tong, Liu & Han, 2002; Tong, 2005; Hulbert *et al.*, 2009; van der Made, 2010; Steiner & Ryder, 2011; Ruiz-García *et al.*, 2016). The resultant time-calibrated phylogeny was used to visually project variation in body mass across *Tapirus*, and statistically to account for the effect of phylogeny on shape data. The first two rPCs for each bone demonstrating size-independence were tested for phylogenetic signal using the 'phytools' and 'geiger' packages (Revell, 2012) in RSTUDIO. Pagel's λ was chosen as a test statistic, with a *P*-value testing for a significant departure from λ = 0 (no correlation between species). Maximum likelihood ancestral states were estimated using the 'phytools' package in RSTUDIO (Revell, 2012, 2013) for all nodes and branches to illustrate variation in body mass across the tree topology (Revell, 2013; Labonte *et al.*, 2016); however, no quantitative or statistical conclusions were drawn from these node estimates. Finally, forelimb shape data across ecological ranges were analysed using phylogenetic multivariate analysis of variance (phyMANOVA), based on species-averaged rPCs accounting for over 70% of shape variation; phyMANOVAs were performed in the RSTUDIO package 'geiger' (Garland *et al.*, 1993). Wilks' lambda (Λ) was calculated for the phyMANOVAs, with associated *F* and *P*-values (significant ≤0.05), and used to test for differences between isotopic group means while simultaneously accounting for phylogenetic relatedness.

RESULTS

Body mass and phylogeny

Body mass calculations for *Tapirus* species in this study are presented in Table 1, with log-transformed body mass ($_{log}$BM) plotted on to the informal phylogenetic tree (Fig. 1). Mass estimates range from the dwarf tapir *T. polkensis* (117 ± 18 kg) to the giant tapir *T.* (*M.*) *augustus* (623 kg). Phylogenetic signal is high for body mass (Pagel's λ > 0.999), although this influence is not statistically significant ($P = 0.155$). Similar results are observed when centroid size and log-transformed centroid size are tested for phylogenetic signal, with no bones significantly deviating from λ = 0 (Table 2; also see Supporting Information, Table S15). Log-transformed centroid size was well correlated with estimated body mass across the forelimb (average $R^2 = 0.70$); $_{log}$CS was, therefore, accepted as a viable proxy for size in the remainder of the study.

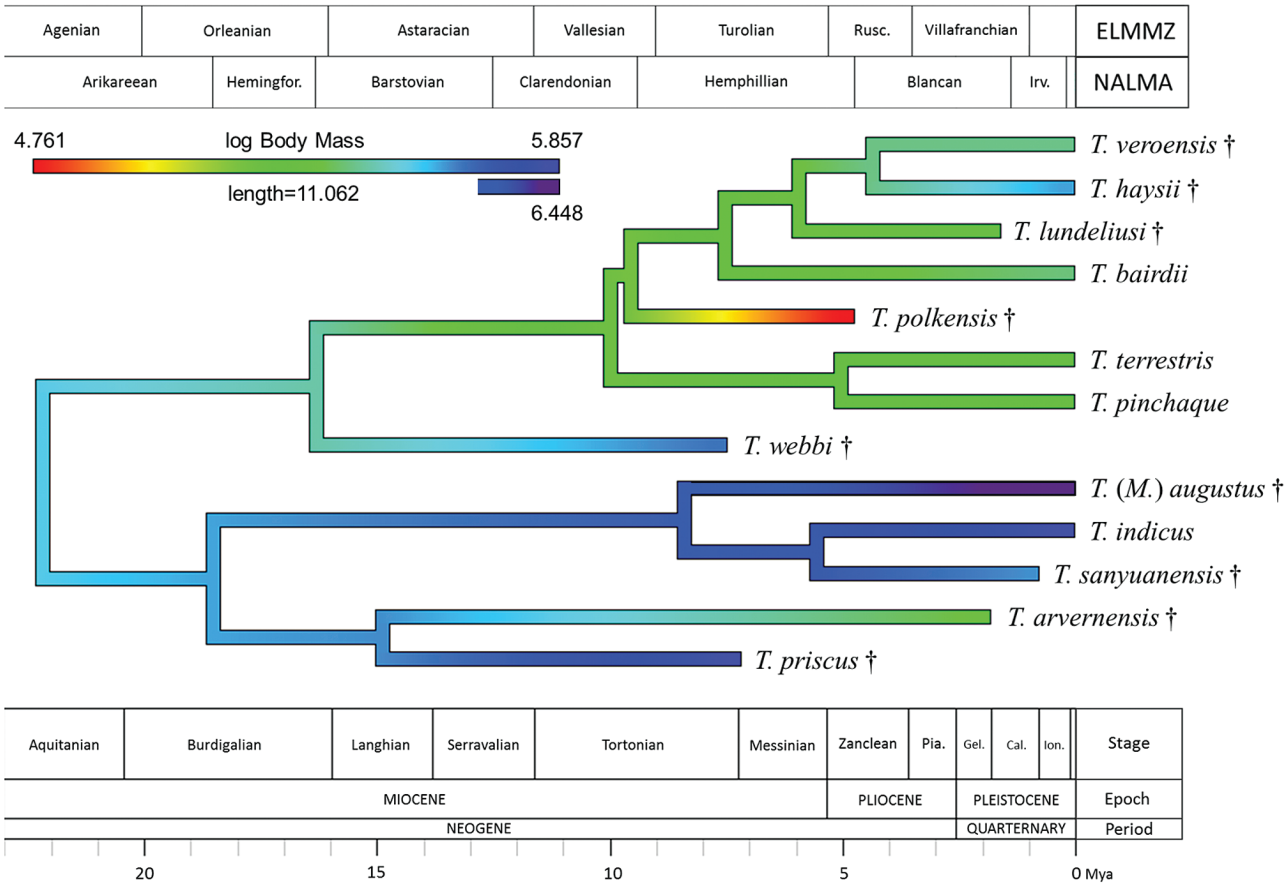

Figure 1. Tapir body mass ($_{log}$BM) plotted onto informal phylogenetic tree. Maximum and minimum trait values shown. Time calibration based upon first-last occurrences. Extinct taxa denoted with †. Outsized *T.* (*M.*) *augustus* plotted with separate scale. Abbreviations of ELMMZ (European Land Mammal Mega-Zones): Rusc., Ruscinian; NALMA, North American Land Mammal Ages; Irv., Irvingtonian; Rancholabrean follows Irvingtonian. Abbreviations of ICS stages: Pia., Piacenzian; Gel., Gelasian; Cal., Calabrian; Ion., 'Ionian'.

Branch length generation from first and last occurrence dates for tapir species in this study suggest that the genus *Tapirus* divided into two geographically separated lineages in the early-middle Aquitanian (~22 Mya), prior to the 'tapir vacuum' (van der Made, 2010). The extinct subgenus *Helicotapirus* (including *T. lundeliusi*, *T. haysii* and *T. veroensis*) is estimated to have split from modern *T. bairdii* around 7 Mya; modern Neotropical taxa are predicted to have diverged 9–10 Mya, with subsequent divergence of *T. terrestris* and *T. pinchaque* lineages around 5 Mya (Fig. 1).

Shape variable regression

Results from multivariate regression of shape variables (Procrustes coordinates) against $_{log}$CS for each bone in this study are presented in Table 3. Half of the bones (six of 12) demonstrated a significant influence of size on the morphology (bold *P*-values; Table 3), most notably in the radius and MCII. The humerus, pisiform, cuneiform, unciform, MCIII and MCIV demonstrate non-significant influence by both $_{log}$CS and $_{log}$BM on the shape variables (Table 3). These bones were further analysed and are described as 'size-independent' bones forthwith. Multivariate regression graphs are displayed in Supporting Information (Fig. S2).

Size-independent shape variation

Size-independent shape variation in the six bones shown to display non-significant allometric influence (humerus, pisiform, cuneiform, unciform, MCIII and MCIV) was examined using principal components analysis of the multivariate regression residuals (Fig. 2). Overall, the extinct North American taxa (*T. webbi*, *T. polkensis*, *T. lundeliusi*, *T. haysii* and *T. veroensis*) cluster in separate regions of morphospace to those of modern Neotropical and Asian species (Fig. 2), although overlaps in morphospace occupation do occur for most bones. Results of phylogenetic signal testing

Table 2. Phylogenetic signal testing on first two principal components of regression residuals and on centroid size (rPC1; rPC2; $_{log}$CS) for species-averaged tapir forelimb bones. Variance % accounted for by each rPC reported, with Pagel's Lambda (λ) and significance of departure from 0 for λ statistic (*P*; significant <0.05). Significant *P*-values for λ statistic in bold; values in italics are *P*-values

Bone	rPC1			rPC2			$_{log}$Centroid Size	
	Var. (%)	λ	*P*	Var. (%)	λ	*P*	λ	*P*
Humerus	54.8	<0.01	*1.00*	18.6	0.85	*0.47*	<0.01	*1.00*
Radius	25.7	0.99	*0.09*	22.7	0.99	*0.13*	0.99	*0.28*
Pisiform	57.6	0.99	***0.04***	18.1	<0.01	*1.00*	0.99	*0.29*
Cuneiform	38.8	<0.01	*1.00*	22.1	<0.01	*1.00*	<0.01	*1.00*
Lunate	37.9	<0.01	*1.00*	19.3	<0.01	*1.00*	0.98	*0.77*
Scaphoid	38.3	<0.01	*1.00*	18.4	<0.01	*1.00*	0.96	*0.560*
Magnum	39.2	<0.01	*1.00*	21.2	<0.01	*1.00*	0.99	*0.52*
Unciform	36.4	0.99	***0.03***	22.4	<0.01	*1.00*	<0.01	*1.00*
Metacarpal II	34.2	0.91	*0.46*	18.8	<0.01	*1.00*	<0.01	*1.00*
Metacarpal III	49.7	<0.01	*1.00*	16.7	0.59	*0.53*	<0.01	*1.00*
Metacarpal IV	48.6	0.99	*0.23*	18.3	<0.01	*1.00*	<0.01	*1.00*
Metacarpal V	44.8	0.99	*0.23*	19.8	<0.01	*1.00*	0.99	*0.51*

Table 3. Multivariate regressions (shape variables vs. size variables) for forelimb bones. Permutation test (×10 000) against a null hypothesis of size-independence (*P*), % sum of squares predicted by size variable (% pred.) reported with significant *P*-values in bold; values in italics are *P*-values

Bone	log Centroid Size		
	N	%pred.	*P*
Humerus	37	5.5	*0.06*
Radius	44	11.9	***<0.01***
Pisiform	46	1.8	*0.54*
Cuneiform	39	2.5	*0.50*
Lunate	47	3.7	***0.03***
Scaphoid	42	5.5	***<0.01***
Magnum	48	5.1	***<0.01***
Unciform	48	3.1	*0.10*
Metacarpal II	51	7.9	***<0.01***
Metacarpal III	50	2.2	*0.15*
Metacarpal IV	45	3.6	*0.10*
Metacarpal V	51	5.3	***<0.01***

for the first two rPCs of all bones are presented in Table 3, with the pisiform and unciform demonstrating significant influence from species' relatedness. PerMANOVA testing suggests overall significant differences in the species' means for all bones (Table 4; see also Supporting Information, Table S2). Pairwise comparisons between species for all bones can be found in the Supporting Information (Tables S3–S14).

In humeral morphospace, the extant mountain tapir *T. pinchaque* is revealed as an outlier to other species (Fig. 2A); the largest taxon in the humeral analysis [*T.* (*M.*) *augustus*] does not cluster with the other large taxa (*T. indicus* and *T. webbi*). The humerus of *T. indicus* is found to be significantly different in size-independent morphology to all taxa in the analysis represented by >1 specimen. Results from phylogenetic signal for the humerus suggest very little influence of interspecific relatedness (rPC1 $\lambda < 0.01$, $P = 1.00$; rPC2 $\lambda < 0.01$, $P = 0.47$).

For pisiform morphospace, the two largest species (*T. indicus* and *T. webbi*) represent the two extremes of morphology along rPC1 (Fig. 2B); *T. webbi* demonstrates a pronounced proximal protrusion of the spatulate process for the insertion of the *m. flexor carpi ulnaris*, causing the process to appear triangular in this species. Pairwise comparisons suggest that the pisiform of *T. webbi* is the most distinct, exhibiting significant differences to all species except *T. haysii*. Of the modern taxa, *T. bairdii* and *T. indicus* demonstrate significant differences ($P = 0.033$), and both *T. indicus* and *T. terrestris* are significantly separated from all extinct species. Phylogenetic signal for the pisiform along rPC1 is high and significantly differs from 0 (rPC1 $\lambda = 0.99$; $P = 0.040$) (Table 4).

Cuneiform morphospace suggests the larger North American species (*T. webbi* and *T. haysii*) exhibit similar morphologies to one another, but divergent from the large Malayan tapir (*T. indicus*) (Fig. 2C). *T. bairdii* displays the greatest difference in cuneiform morphology to other taxa, with significant differences found between it and all taxa represented by >1 specimen.

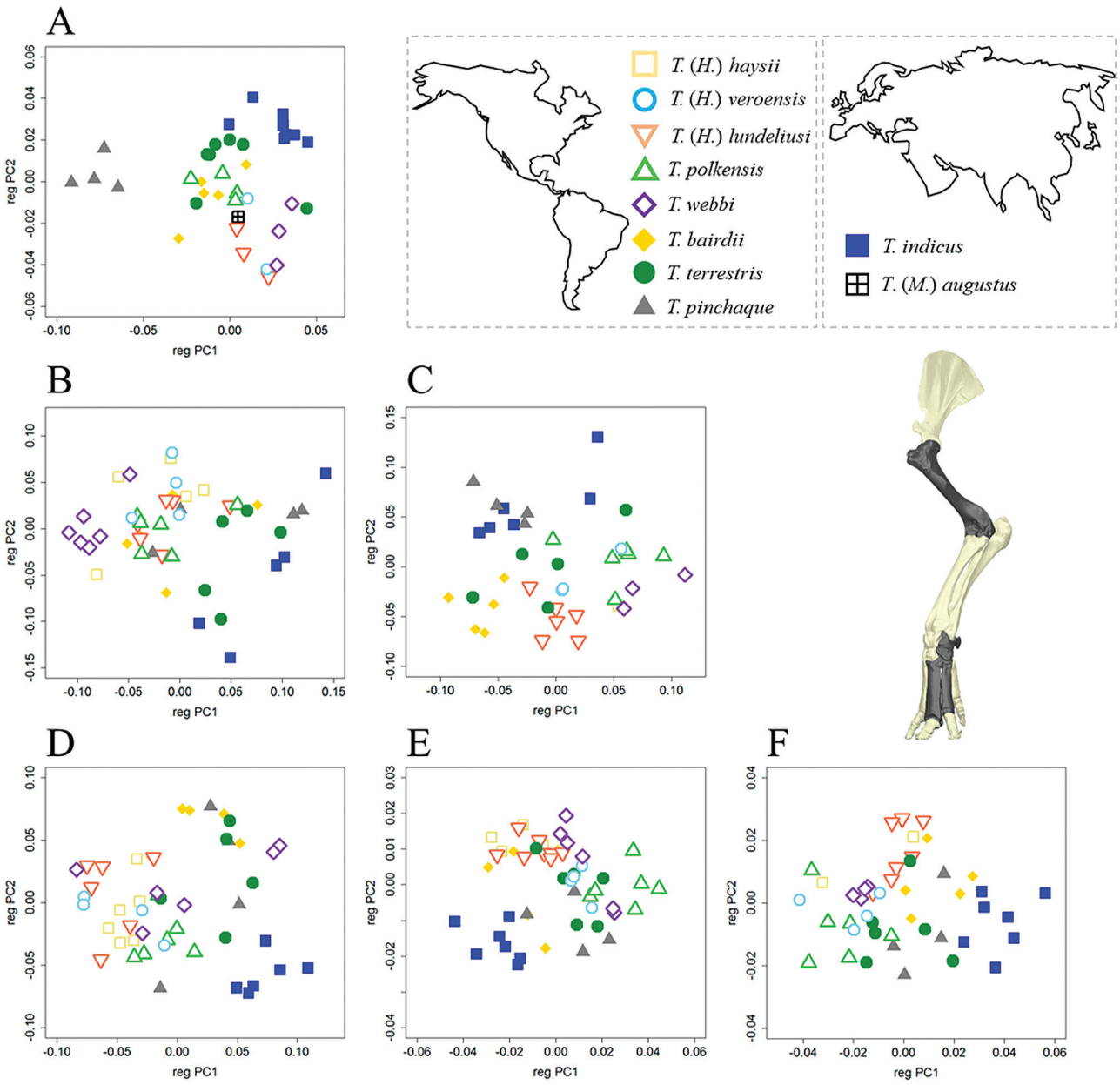

Figure 2. Morphospace occupation based on multivariate regression residuals (shape vs. log-transformed centroid size) for six *Tapirus* forelimb bones: A, humerus; B, pisiform; C, cuneiform; D, unciform; E, metacarpal III; F, metacarpal IV. Representative bones are shown in situ on left forelimb of *T. bairdii* (RMNH 43495).

Phylogenetic signal for the cuneiform is very low (rPC1 $\lambda < 0.01$; rPC2 $\lambda < 0.01$) (Table 3); along with the humerus, the cuneiform displays the least influence from both body mass and species' relatedness.

The spread of species in unciform morphospace suggests a splitting of taxa into three groups with minimal overlap: a *T. indicus* group, an extant Neotropical grouping and a North American group (Fig. 2D); two *T. webbi* are removed from the main North American group. The unciform displays significant phylogenetic signal for rPC1 ($\lambda > 0.99$; $P = 0.03$), but not for rPC2 ($\lambda < 0.01$).

Metacarpal III (MCIII) morphospace patterns show the greatest degree of overlap between extant and extinct species (Fig. 2E). The only Eurasian taxon (*T. indicus*) plots separately to all New World tapirs. *T. webbi* possesses the largest MCIIIs, and is the only taxon to exhibit non-significant differences in MCIII morphology (to *T. pinchaque*, *T. terrestris* and

Table 4. PerMANOVAs of *Tapirus* species based on regression residuals for six forelimb bones corrected for false discovery rate (10 000 permutations). Sum of squares and within-group sum of squares reported alongside *F*-statistic (*F*) and associated *P*-values (*P*). Significant differences in bold; values in italics are *P*-values

Bone	Perm.	Sum of squares	Within group sum	*F*	*P*
Humerus	10000	0.116	0.051	4.400	***<0.001***
Pisiform	10000	0.578	0.364	2.714	***<0.001***
Cuneiform	10000	0.513	0.295	2.772	***<0.001***
Unciform	10000	0.581	0.349	3.249	***<0.001***
Metacarpal III	10000	0.059	0.031	4.661	***<0.001***
Metacarpal IV	10000	0.077	0.042	3.722	***<0.001***

Table 5. One-way analysis of variance (ANOVA) comparing raw stable isotopic values within ranges, with Tukey's pairwise comparisons. Average values on the border of two ranges (e.g. *T. webbi* $\delta^{13}C = -13‰$) are placed in the more depleted range (e.g. *T. webbi* within range 2). Tukey's Q below pairwise diagonal and *P*-values above the diagonal; significant *P*-values in bold; values in italics are *P*-values

Test	Sum of squares	DF	*F*	*P*
Equal Means	135.328	3.00	39.78	***<0.001***
Welch *F* test	-	44.5	34.11	***<0.001***
Group	dry open canopy	wet open canopy	closed canopy	dense canopy
dry open canopy		*0.277*	***<0.001***	***<0.001***
wet open canopy	2.56		***<0.001***	***<0.001***
closed canopy	9.99	7.44		***0.044***
dense closed canopy	13.76	11.21	3.77	

T. veroensis). Phylogenetic signal for the MCIII is overall low (rPC1 $\lambda < 0.01$; rPC2 $\lambda = 0.59$).

Metacarpal IV (MCIV) morphospace occupation suggests a gradual size-independent shape difference spectrum from North American taxa, through South American taxa to Eurasian taxa along rPC1 (Fig. 2F). *T. webbi* and *T. haysii* occupy different regions of morphospace to the equally large *T. indicus*. Both *T. indicus* and *T. bairdii* differ significantly from all other tapirs in the analysis, with *T. webbi* and *T. lundeliusi* exhibiting significant differences to all other taxa except *T. haysii*. Phylogenetic signal for the MCIV is high (rPC1 $\lambda = 0.99$; rPC2 $\lambda < 0.01$), suggesting that patterns of morphospace occupation along rPC1 for this bone are heavily influenced by phylogenetic relationships.

Shape and habitat variation

One-way ANOVA results comparing habitat mean and species mean $\delta^{13}C$ values demonstrated overall significant differences between group means ($P < 0.01$; Table 5; species' means in Supporting Information, Table S16); post hoc Tukey's pairwise differences are also listed in Table 5. PhyMANOVA results comparing shape data across isotopic ranges (habitat proxy) are reported in Table 6. Two out of the six bones examined (MCIII and MCIV) demonstrated no significant differences in morphology across the habitat gradient. Three of the remaining bones (all carpals: pisiform, cuneiform and unciform) demonstrated significant differences in morphology across the habitat gradient prior to phylogenetic correction (Table 6). Following correction for phylogeny, these bones continued to exhibit morphological differences across the habitat density gradient (corrected $P = 0.051–0.072$; Table 6). Additional testing of two subsets of data (all bones subset and New World species' subset) did not greatly differ from results in the initial analysis, although the morphology of the size-dependent second metacarpal was shown to be significantly different across the habitat gradient (Supporting Information, Tables S17–S18). The lunate, scaphoid (proximomedial carpus) and the fifth metacarpal (lateral autopodium) also demonstrate significant differences in the New World subset (Supporting Information, Table S18).

DISCUSSION

In this study, we used estimates of body mass, phylogenetic relationships and quantitative three-dimensional shape analysis to test whether forelimb variation observed in tapirs is purely an artefact of body size (as suggested by: Hershkovitz, 1954; Radinsky, 1965; and many subsequent authors), or whether differences in

Table 6. phyMANOVAs of size-independent shape variables against average stable carbon isotope ($\delta^{13}C$) ranges, based on rPC scores accounting for >70% variance of species averaged shape data (10 000 simulations). Significant values for Wilks' Lambda statistic (Λ) and associated *P*-value (*P*) and phylogenetically corrected *P*-values (corr. *P*) are in bold; values in italics are *P*-values

Bone	DF	Λ	*F*	*P*	corr. *P*
Humerus	3	0.060	3.078	*0.099*	*0.054*
Pisiform	3	0.050	4.605	***0.026***	*0.066*
Cuneiform	3	0.009	4.842	***0.022***	*0.051*
Unciform	3	0.012	4.225	***0.031***	*0.072*
Metacarpal III	3	0.099	1.315	*0.362*	*0.587*
Metacarpal IV	3	0.079	1.519	*0.291*	*0.494*

habitat have influenced morphology in the postcranial skeleton of *Tapirus*. We demonstrate that habitat does influence forelimb shape variation in tapirs after allometry (size-dependent shape) is accounted for, hence refuting previous claims of obligate size-dependence in tapir limb morphology. Due to the fact that we incorporated extinct taxa in this experiment, it is important that abiotic influences on fossilized bone shape be addressed. Specimen descriptions and excavation accounts from fossiliferous sites in Florida and Tennessee (including Gray Fossil Site, Love Bone Bed, Leisey Shell Pit and Haile 7 sites, among others; Hulbert *et al.* 2006, 2009; Hulbert 2010) report exceptional preservation of three-dimensional structures of vertebrate remains, including that of numerous tapir species. Accordingly, we reject the notion that differences in morphospace occupation observed in extant and extinct tapirs are caused by post-mortem deformation. The limited postcranial remains available for this study from Eurasian and extinct South American *Tapirus* species should also be noted as an unfortunate drawback of the analysis. The results of morphological comparisons of the radius suggest that European taxa resemble one another more greatly than they do other Asian or American taxa; this result is not highlighted in the main discussion as it is based on only one bone from two species (*T. priscus* and *T. arvernensis*). Nevertheless, expanding the sample of scanned tapir limbs to include more European, Asian and American specimens has the potential to greatly improve resolution and the biogeographical scope of the results presented here. Despite these methodological limitations, tapir body sizes observed in this study provide a perfect range for testing the hypotheses laid out by the authors. Hereafter we discuss the results of biotic influences on tapir forelimb morphology in relation to fluctuations in body size and variation in habitat.

Size-independence in forelimb shape

The historical viewpoint on tapir postcranial variation suggests that the limbs have remained basically unchanged, with any modifications resulting from changes in size (Hershkovitz, 1954; Radinsky, 1965; Padilla *et al.*, 2010). We demonstrate that 50% of bones from the forelimb of tapirs exhibit no significant influence of size on morphological variation (six of 12 bones; scapula, trapezoid, trapezium and phalanges excluded) (Table 2; Fig. 2). Our morphospace results, based on bones demonstrating no significant influence of size on shape (Fig. 2), demonstrate a number of interspecific groupings implying differences between *Tapirus* taxa independent of size effects.

In the humerus we observe *T. pinchaque* as an outlier in morphospace (Fig. 2A). This is likely as a result of adaptations for increased speed of shoulder flexion (detailed in: MacLaren & Nauwelaerts, 2016). We also observe that the giant Asian tapir *T.* (*Megatapirus*) *augustus* does not plot near to its closest relative (*T. indicus*) in morphospace, but rather is found proximate to *Helicotapirus* taxa and *T. webbi*. These North American tapirs demonstrate large but less robust humeri than *T. indicus*. Rather than exhibiting similar limb morphology to other large-bodied tapirs, *T. indicus* in fact represents a highly robust morph of *Tapirus*, demonstrating significant differences in shape to other large tapirs with limbs of similar or greater absolute size (e.g. *T. haysii* and *T. webbi*) (Supporting Information, Tables S3–S14).

Previous observations on the size of the limbs in *T. webbi* (Hulbert, 2005) are supported by centroid size results in this study. In our morphospace results, *T. webbi* is frequently observed occupying regions proximal to *T. polkensis* (Fig. 2; hollow triangles and hollow diamonds). These tapirs are both Miocene in age (Fig. 1) and, although they are phylogenetically separated, they share several morphological features of the forelimb. Shared features include a prominent process on the pisiform for insertion of flexor tendons, an emarginated scapho-lunate joint facet (primitive feature for Perissodactyla; Holbrook, 1999), and long and relatively slender metacarpals. The large and long-limbed *T. webbi* is in many cases more comparable in form to

other North American tapirs rather than to similarly large tapirs from Eurasia (e.g. *T. indicus* and *T. priscus*) (Supporting Information, Tables S3–S14). This result would not be expected were tapir limb morphology influenced solely by size. Body mass estimates for *T. webbi* (293 ± 31 kg) do suggest it is, on average, smaller than large Eurasian species such as *T. indicus* (326 ± 14 kg), thus morphological differences are to be expected; however, we also find evidence for a decoupling of mass and morphology in the forelimb of two small tapir taxa of essentially equal estimated body mass: *Tapirus lundeliusi* and *T. pinchaque*.

Decoupling mass and morphology in Tapirus

During the process of body mass estimation, two taxa presented comparable average body masses: the Early Pleistocene *Tapirus lundeliusi* from Florida (202 ± 24 kg) and the extant mountain tapir *T. pinchaque* (202 ± 19 kg; Fig. 3A). Despite similar mass estimates, *T. lundeliusi* and *T. pinchaque* are statistically separated from one another in forelimb bone shape (Supporting Information, Table S3–S13). These two species represent an ideal example of divergent morphologies irrespective of size in the forelimb of *Tapirus*. We find that several features previously shown to be of adaptive advantage for *T. pinchaque* (MacLaren & Nauwelaerts, 2016) contribute greatly to the distinction from *T. lundeliusi* (Supporting Information, Tables S3–S8). Shoulder flexor muscle insertions proximal to the humeral head suggest more rapid shoulder flexion in *T. pinchaque*, at the expense of power (Gambaryan, 1974; Hildebrand, 1985; MacLaren & Nauwelaerts, 2016). When combined with the gracile morphology of the proximal limb bones, this feature implies that *T. pinchaque* is capable of more rapid upper forelimb flexion than the extinct *T. lundeliusi*. The humerus of *T. pinchaque* displays greater torsion than *T. lundeliusi*, reducing supination of the entire forelimb at the shoulder (Fig. 3B) and bringing

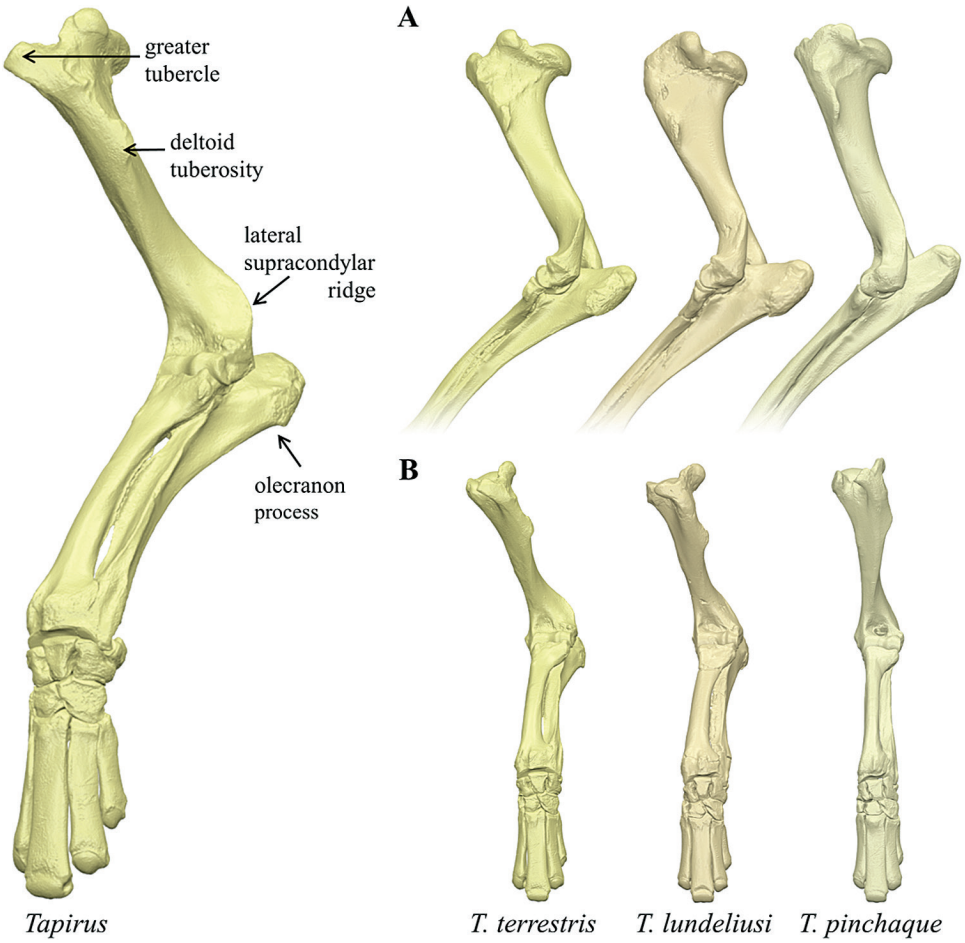

Figure 3. Forelimb morphology in three tapir species of comparable body masses. Full forelimb of *Tapirus* alongside (A) elbow morphology in lateral view and (B) stylopodial profile in frontal view (manus fixed in identical orientation). Specimens: *T. terrestris* ZMB MAM 12999 (216.5 kg); *T. lundeliusi* UF 121736 (202.8 kg); *T. pinchaque* ZMB MAM 62085 (202.4 kg).

the entire forelimb into the parasagittal plane (associated with increased cursoriality: Gregory 1929; Wood *et al.*, 2010). We hereby highlight a further adaptation toward a divergent locomotor style in the forelimb of *T. pinchaque* that has been previously discussed (MacLaren & Nauwelaerts, 2016, 2017).

Overall, forelimb morphology in *T. lundeliusi* is more in keeping with New World tapirs exhibiting much greater body mass than predicted for this taxon in the present study. *T. lundeliusi* exhibits more distally placed shoulder flexors and a posteriorly deflected olecranon process than *T. pinchaque* (MacLaren & Nauwelaerts, 2016), features enabling *T. lundeliusi* to bear greater loads at the shoulder and elbow joints. A thickened proximal humerus (Fig. 3A), distally positioned deltoid tuberosity (Fig. 3A, B) and posteriorly deflected olecranon process (Fig. 3A), all imply that the forelimb of the Florida endemic *T. lundeliusi* was adapted for slow and powerful shoulder flexion, and potentially greater gravitational support than tapirs of similar (and sometimes greater) predicted body mass (e.g. *T. terrestris*, *T. bairdii*, *T. veroensis* and *T. pinchaque*) (Gregory, 1929; Hermanson & MacFadden, 1992; MacLaren & Nauwelaerts, 2016, 2017). In addition to features of the forelimb highlighted in this study (e.g. thickened humeral shaft, deflected olecranon and locked cuneiform–pisiform joint), *T. lundeliusi* demonstrates a series of primitive cladistic characteristics of the skull (including long nasals and a short maxilliary flange) (Hulbert, 1995, 2010). We suggest that the upper arm morphology and cuneiform–pisiform interaction are plesiomorphic for the *Helicotapirus* clade, lost in the youngest taxon (*T. veroensis*).

When compared to medium-sized tapirs (e.g. *T. bairdii*, *T. terrestris* and *T. veroensis*), *T. lundeliusi* displays upper limb and lateral carpal adaptations in keeping with a taxon of much higher mass (MacLaren & Nauwelaerts, 2016), with thicker bones and more tightly locked carpal joints than is evident in the largest modern tapir (*T. indicus*). Contrastingly, *T. pinchaque* demonstrates a suite of features associated with rapid limb flexion and shock absorption (MacLaren & Nauwelaerts, 2016, 2017). These two small taxa perfectly demonstrate that tapirs of comparable size display species-specific adaptations to the forelimb to suite their individual biological requirements, challenging the historical perspective of size-dependent postcranial disparity.

Manus variation across habitat gradient

This study compliments previous findings by demonstrating that limb disparity in tapirs is affected by intrinsic (e.g. phylogeny) and extrinsic (e.g. environmental) factors in combination with fluctuations in body size (MacLaren & Nauwelaerts, 2016, 2017). One extrinsic factor, habitat density, was here shown to affect tapir forelimb morphology to a more significant extent than was expected, given the restricted niche occupied by modern tapirs. The general ecological role of tapirs in modern ecosystems is well documented (Gregory, 1929; MacFadden & Hulbert, 1990; Downer, 2001; DeSantis & MacFadden, 2007; Perez-Crespo *et al.*, 2012; de Thoisy *et al.*, 2014; Bocherens *et al.*, 2017; Stacklyn *et al.*, 2017). Extant tapirs represent medium-to-large crepuscular and nocturnal browsers, existing in low densities within wet, tropical biomes (Padilla & Dowler, 1994; Padilla *et al.*, 2010; Ruiz-García *et al.*, 2012; de Thoisy *et al.*, 2014). It is evident from this study and others (MacFadden & Hulbert, 1990; Czaplewski *et al.*, 2002; Graham, 2003; DeSantis & Wallace, 2008) that tapirs have not always been restricted to dense rainforest habitats, as demonstrated by stable carbon ($\delta^{13}C$) isotopic values.

Levels of $\delta^{13}C$ in tooth enamel are indicative of the proportion of C3 and C4 plant material in the diet (Cerling *et al.*, 1997; Cerling, Harris & Leakey, 1999; Cerling, Hart & Hart, 2004; DeSantis & MacFadden, 2007). Values above –9‰ suggest mixed C3/C4 diet, with higher values suggestive of a drier and more open habitat. Stable carbon isotopic values of –13‰ to –10‰ have been shown to represent open-canopy forest, with less depleted values demonstrating decreasing moisture available for vegetation (Ehleringer *et al.*, 1987; Mooney, Bullock & Ehleringer, 1989; Codron *et al.*, 2005; Secord *et al.*, 2008). Values of $\delta^{13}C$ more depleted than –14‰ strongly suggest a closed-canopy tropical biome (Cerling *et al.*, 2004; Codron *et al.*, 2005; Secord *et al.*, 2008).

When stable carbon isotope recordings for modern and extinct tapirs are compared, both the average and range of $\delta^{13}C$ show dense forest environments for modern tapir taxa (Fig. 4; Table S16). The most depleted $\delta^{13}C$ values in this study are found in the modern *T. terrestris* (average = –15.6‰) and *T. indicus* (average = –15.4‰); these values are equivalent to those of other extant rainforest browsers, such as duikers (Cephalophinae) and chevrotains (Tragulidae) in Central Africa (Cerling *et al.*, 2004) and banteng in South China (Qu *et al.*, 2014; Bocherens *et al.*, 2017). By contrast, the least depleted average $\delta^{13}C$ value is that of *T. haysii* (average = –12.2‰), including a population from Mexico exhibiting $\delta^{13}C$ values averaging –10.7‰ (Perez-Crespo *et al.*, 2016). Similar $\delta^{13}C$ values are reported for white-tailed deer *Odocoileus* (–12.1‰; MacFadden & Cerling, 1996), red deer *Cervus elaphus* (–11.4‰; Garcia *et al.*, 2009) and the European forest horse *Equus germanicus* (–11.7‰; Scherler *et al.*, 2014), all of which are regarded as open-woodland taxa existing in temperate forest biomes. The average isotopic values for *T. haysii* also approximate that of the gracile Oligocene tapir *Colodon* (–12.2‰)

from the White River fauna in Nebraska (Boardman & Secord, 2013), suggested as the first representation of tapiromorphs exploiting riparian refugia within an otherwise dry, open habitat (Zanazzi & Kohn, 2008; Boardman & Secord, 2013). This may also be the case for the Pleistocene tapirs *T. haysii* and *T. veroensis* (–12.7‰), whose ranges include habitats proximate to the continental glacial front during the Pleistocene ice age (Czaplewski *et al.*, 2002; Graham, 2003), and represent a drier habitat than that typical of modern tapirs. The forest environments inhabited by these Pleistocene tapirs would have been composed of different flora, likely with a reduced canopy coverage (as indicated by the more enriched $\delta^{13}C$ values; Fig. 4). Variation in forest density (i.e. canopy cover) is a vital factor for a large-bodied ungulate negotiating its way through its environment, potentially limiting size and locomotor style (Curran, 2015). In this study we found not only that extinct tapir species inhabit less dense forest environments (Fig. 4), but also that the morphology of the lateral manus is significantly different across the forest density gradient (Table 6; see also Supporting Information, Tables S17–S18).

In this study we reveal that the lateral carpus (consisting of the pisiform, cuneiform and unciform carpals) exhibits significant morphological variation in tapirs across a habitat density gradient (Table 6). Despite phylogenetic correction elevating corrected *P*-values above the threshold of 0.05 for the pisiform ($P = 0.066$), cuneiform (0.051) and unciform (0.072) (Table 6), we believe that the morphological signal these bones demonstrate between ecological groups is worthy of recognition and discussion. These carpals are all located on the lateral autopodium, a region previously highlighted as being of morphological interest in modern tapir species (Earle, 1893; Simpson, 1945; MacLaren & Nauwelaerts, 2016, 2017). For example, both *T. indicus* and *T. pinchaque* possess an expanded unciform joint facet for the lateral metacarpals than either *T. terrestris* or *T. bairdii*; this adaptation implies greater reliance on the fifth metacarpal in *T. pinchaque* and *T. indicus* than in other extant taxa (MacLaren & Nauwelaerts, 2017). When we consider the position in morphospace of the extinct *Helicotapirus* species (the three taxa with highest carbon isotopic values), both the pisiform and unciform of these taxa are greatly separated from the isotopically depleted *T. indicus* and *T. terrestris* (Fig. 2B, D). There has been little research into the effect of habitat differences on carpal morphology within ungulate clades. One previous investigation into the carpus of cervids in relation to habitat use found no direct evidence for morphological differences in the carpal complex between closed and open habitat (Schellhorn & Pfretzschner, 2014).

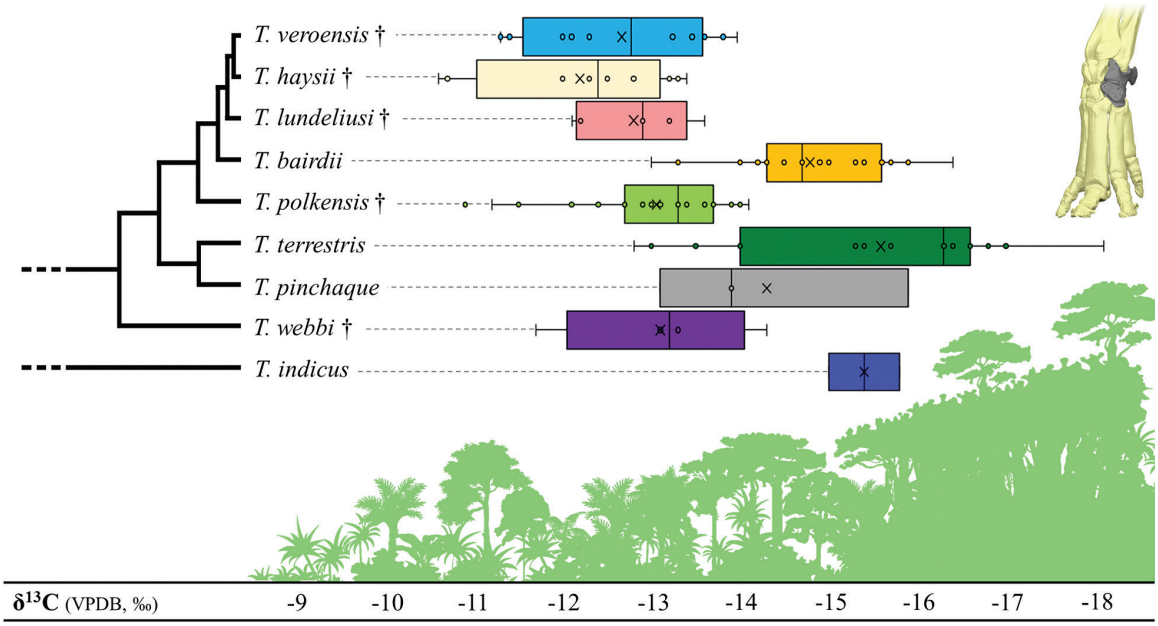

Figure 4. Stable carbon isotope ranges across *Tapirus*. Composite phylogeny of taxa (left) in this study alongside diagrammatic canopy cover (bottom) with corresponding stable carbon isotopic levels, and manus bones exhibiting significant differences between isotopic ranges (top right). X = mean value; central bar = median; filled boxes denotes 50% between first and third quartiles. Isotope values from: MacFadden & Cerling, 1996; Koch *et al.*, 1998; Kohn *et al.*, 2005; Hoppe & Koch, 2006; DeSantis & Wallace, 2008; DeSantis *et al.*, 2009; DeSantis, 2011; Perez-Crespo *et al.*, 2012. Treeline design after Arini lighting (www.hess.eu).

In the present study, however, we do identify differences in morphology of the lateral carpus across a habitat density gradient. The unciform demonstrates a trend towards a relatively increased cuneiform facet in more open-woodland taxa; accordingly, the cuneiform facet for the unciform is more elongate anteroposteriorly in tapirs inhabiting less dense woodland. In addition, the pisiform facet becomes relatively smaller, more posteriorly deflected and more laterally positioned as tapirs inhabit denser forest habitats. Finally, the ulnar joint facet on the pisiform becomes gradually more asymmetrical as taxa are found in denser habitats, with a strong medial process present in dense-habitat tapirs compared to an elliptical facet found in open-woodland taxa. As these three bones are closely associated, it may not be surprising that they all demonstrate significant differences across the habitat gradient prior to phylogenetic corrections. The change in significance values between phylogenetically corrected and non-corrected *P*-values across the habitat groups may be explained by monophyly of the *Helicotapirus* clade (*T. haysii*, *T. lundeliusi* and *T. veroensis*). The *Helicotapirus* tapirs demonstrate morphological divergence in the lateral carpus (in particular the cuneiform), in addition to being the only tapir taxa in this analysis with average $\delta^{13}C$ values greater than –13‰ (Koch *et al.*, 1998; Kohn *et al.*, 2005; Hoppe & Koch, 2006; DeSantis *et al.*, 2009).

From the data currently available, formulating direct functional outcomes from the morphological variation observed across the habitat density gradient would require an over-interpretation of the findings. Unfortunately, a lack of stable carbon isotopic and extensive morphological data for European tapirs, including *T. priscus*, *T. arvernensis* and others, prevented these taxa playing a greater role in this analysis. Increased taxon and specimen counts, additional palaeoenvironmental data (e.g. stable oxygen isotopes, widespread palaeobotanical assessments, etc.) and digital simulations or *in vivo* experiments on the functional morphology of the carpal complex in tapirs will be necessary before more conclusive interpretations can be made on the influence of habitat density on the tapir forelimb. The isotopic signal in this study is intriguing, and promotes future studies to compare morphological and habitual data in this fashion.

CONCLUSION

Using a size-independent, three-dimensional approach to quantify forelimb shape, we have shown that the forelimb of *Tapirus* demonstrates notable variation not significantly influenced by size. As part of this study, we present the first published body mass estimates for several *Tapirus* species [including *T.* (*Megatapirus*) *augustus*, *T. priscus*, *T. lundeliusi*, *T. veroensis* and *T. arvernensis*], the results of which suggest that Eurasian tapirs attained greater masses on average than those in the Americas. Addition of extinct tapir specimens from southern Europe, China and South America may offer greater resolution to this apparent geographical variation. Our findings highlight an apparent decoupling of tapir size and limb morphology, highlighted by two small taxa of near-equal estimated mass (*T. pinchaque* and *T. lundeliusi*). We observe previously overlooked adaptations in the forelimb skeleton of the modern mountain tapir, *T. pinchaque*, shedding further light on the divergent locomotor capabilities of this elusive and endangered taxon. Variation across an ecological gradient is observed in the lateral autopodium of *Tapirus*. The confounding influence of phylogenetic relatedness suggests that morphological variation observed in the lateral autopodium may be driven by tapirs in the subgenus *Helicotapirus*, which in general occupied drier and more open woodland habitat than their modern rainforest relatives.

The sample of taxa used in this study all fall within the genus *Tapirus*, which, while being a deep-rooted clade, does not account for all morphologies within the Tapiridae or Tapiromorpha. To gain a holistic viewpoint on postcranial scaling in tapirs throughout their evolutionary history, further investigation into body size, limb proportions, habitat ecology and locomotor capabilities must be carried out on multiple extinct tapiromorphs outside crown Tapiridae (e.g. *Heptodon*, *Colodon* and *Protapirus*). Understanding the locomotor capabilities of these early taxa, prior to the origination of crown Tapiridae, will expose further insights into this bizarre clade of browsing ungulates and their plesiomorphic, yet variable, locomotor apparatus.

ACKNOWLEDGEMENTS

The authors would like to thank E. Hoeger and J. Meng (AMNH), C. Widga (ETMNH), L. Tyteca (MEO), J. Lésur (MNHN), C. Conroy (MVZ), F. Zachos (NHMW), P. Kamminga and S. Van er Mije (RMNH), C. Funk and S. Bock (ZMB) for provision of museum specimens, and L. DeSantis for tapir isotope values. JM would like to personally thank N. Tomsin and H. Hanegraef (scanning), J. Meaney-Ward and J. Pirlo (logistics), and C. and D. Leiske (personal support). The authors wish to thank two anonymous reviewers for their helpful and constructive comments. This study was financially supported by an FWO doctoral fellowship and FLMNH International Travel Grant (JM) and BOF-UA grant (SN).

REFERENCES

Anderson MJ. 2001. A new method for non-parametric multivariate analysis of variance. *Austral Ecology* **26:** 32–46.

Bai B, Meng J, Wang YQ, Wang HB, Holbrook LT. 2017. Osteology of the middle Eocene ceratomorph *Hyrachyus modestus* (Mammalia, Perissodactyla). *Bulletin of the American Museum of Natural History* **413:** 1–70.

Bapst DW. 2012. Paleotree: an R package for paleontological and phylogenetic analyses of evolution. *Methods in Ecology and Evolution* **3:** 803–807.

Benjamini Y, Hochberg Y. 1995. Controlling the false discovery rate: a practical and powerful approach to multiple testing. *Journal of the Royal Statistical Society. Series B (Methodological)*: 289–300.

Boardman GS, Secord R. 2013. Stable isotope paleoecology of White River ungulates during the Eocene–Oligocene climate transition in northwestern Nebraska. *Palaeogeography, Palaeoclimatology, Palaeoecology* **375:** 38–49.

Bocherens H, Schrenk F, Chaimannee Y, Kullmer O, Morike D, Pushinka D, Jaeger JJ. 2017. Flexibility of diet and habitat in Pleistocene South Asian mammals: implications for the fate of the giant fossil ape Gigantopithecus. *Quaternary International* **434:** 148–155.

Cerling TE, Harris JM, Ambrose SH, Leakey MG, Solounias N. 1997. Dietary and environmental reconstruction with stable isotope analyses of herbivore tooth enamel from the Miocene locality of Fort Ternan, Kenya. *Journal of Human Evolution* **33:** 635–650.

Cerling TE, Harris JM, Leakey MG. 1999. Browsing and grazing in elephants: the isotope record of modern and fossil proboscideans. *Oecologia* **120:** 364–374.

Cerling TE, Hart JA, Hart TB. 2004. Stable isotope ecology in the Ituri Forest. *Oecologia* **138:** 5–12.

Codron J, Codron D, Lee-Thorp JA, Sponheimer M, Bond WJ, de Ruiter D, Grant R. 2005. Taxonomic, anatomical, and spatio-temporal variations in the stable carbon and nitrogen isotopic compositions of plants from an African savanna. *Journal of Archaeological Science* **32:** 1757–1772.

Colbert MW. 2005. The facial skeleton of the early Oligocene *Colodon* (Perissodactyla, Tapiroidea). *Palaeontologia Electronica* **8:** 1–27.

Colbert EH, Hooijer DA. 1953. Pleistocene mammals from the limestone fissures of Szechwan, China. *Bulletin of the American Museum of Natural History* **102:** 1–134.

Curran SC. 2015. Exploring *Eucladoceros* ecomorphology using geometric morphometrics. *Anatomical Record (Hoboken, N.J.: 2007)* **298:** 291–313.

Czaplewski NJ, Puckette WL, Russell C. 2002. A Pleistocene tapir and associated mammals from the southwestern Ozark Highland. *Journal of Cave and Karst Studies* **64:** 97–107.

Damuth J, MacFadden BJ. 1990. *Body size in mammalian paleobiology: estimation and biological implications*. Cambridge: Cambridge University Press, 1–142.

DeSantis LRG. 2011. Stable isotope ecology of extant tapirs from the Americas. *Biotropica* **43:** 746–754.

DeSantis LRG, MacFadden BJ. 2007. Identifying forested environments in deep time using fossil tapirs: evidence from evolutionary morphology and stable isotopes. *Courier-Forschungsinstitut Senckenberg* **258:** 147–157.

DeSantis LRG, Wallace SC. 2008. Neogene forests from the Appalachians of Tennessee, USA: geochemical evidence from fossil mammal teeth. *Palaeogeography, Palaeoclimatology, Palaeoecology* **266:** 59–68.

DeSantis LRG, Feranec RS, MacFadden BJ, Robinson T, Roeder B. 2009. Effects of global warming on ancient mammalian communities and their environments (J Moen, ed.). *PLoS ONE* **4:** e5750.

Downer CC. 2001. Observations on the diet and habitat of the mountain tapir (*Tapirus pinchaque*). *Journal of Zoology* **254:** 279–291.

Earle C. 1893. Some points in the comparative osteology of the tapir. *Science (New York, N.Y.)* **21:** 118.

Ehleringer JR, Lin ZF, Field CB, Sun GC, Kuo CY. 1987. Leaf carbon isotope ratios of plants from a subtropical monsoon forest. *Oecologia* **72:** 109–114.

Eisenmann V, Guérin C. 1992. *Tapirus priscus* kaup from the upper Miocene of Western Europe: palaeontology, biostratigraphy and palaeoecology. *Paleontologia i Evolucio* **24–25:** 113–122.

Feranec RS, MacFadden BJ. 2006. Isotopic discrimination of resource partitioning among ungulates in C_3 -dominated communities from the Miocene of Florida and California. *Paleobiology* **32:** 191–205.

Gambaryan PP. 1974. *How mammals run: anatomical adaptations*. New York: John Wiley & Sons.

Garcia NG, Feranec RS, Arsuaga JL, Bermudez de Castro JM, Carbonell E. 2009. Isotopic analysis of the ecology of herbivores and carnivores from the Middle Pleistocene deposits of the Sierra De Atapuerca, northern Spain. *Journal of Archaeological Science* **36:** 1142–1151.

Garland T, Dickerman AW, Janis CM, Jones JA. 1993. Phylogenetic analysis of covariance by computer simulation. *Systematic Biology* **42:** 265–292.

Graham RW. 2003. Pleistocene tapir from Hill Top Cave, Trigg County, Kentucky, and a review of Plio-Pleistocene tapirs of North America and their paleoecology. In: Schubert BW, Mead JI, Graham RW, eds. *Ice age cave faunas of North America*. Indianapolis: Indiana University Press, 87–118.

Gregory WK. 1929. Mechanics of locomotion in the evolution of limb structure as bearing on the form and habits of the titanotheres and the related odd-toed ungulates. In: Osborn HF, ed. *The titanotheres of ancient Wyoming, Dakota and Nebraska*. Washington DC: United States Government Printing Office, 727–756.

Guérin C, Eisenmann V. 1982. Répartition stratigraphique des tapirs (Mammalia, Perissodactyla) dans le Néogène et le Quaternaire d'Europe occidentale. *IXeme Réunion Annuelle des Sciences de la Terre, Societe Geologique de France*. 298.

Hammer Ø, Harper DAT, Ryan PD. 2001. PAST: paleontological statistics software package for education and data analysis. *Palaeontologia Electronica* **4:** 9.

Hermanson JW, MacFadden BJ. 1992. Evolutionary and functional morphology of the shoulder region and

stay-apparatus in fossil and extant horses (Equidae). *Journal of Vertebrate Paleontology* **12:** 377–386.

Hershkovitz P. 1954. Mammals of Northern Colombia, Preliminary Report No. 7: Tapirs (genus *Tapirus*) with a systematic review of American species. *Proceedings of the United States National Museum* **103:** 465–496.

Hervé M. 2016. *Aide-mémoire de statistique appliquée à la biologie: Constuire son étude et analyser les résultats à l'aide du logiciel R*: 1–203.

Hildebrand M. 1985. Walking and running. In: Hildebrand M., Bramble DM., Liem KF., Wake DB, eds. *Functional vertebrate morphology*. Cambridge: Harvard University Press, 38–57.

Holanda EC, Ferrero BS. 2013. Reappraisal of the genus *Tapirus* (Perissodactyla, Tapiridae): systematics and phylogenetic affinities of the South American tapirs. *Journal of Mammalian Evolution* **20:** 33–44.

Holbrook LT. 1999. The phylogeny and classification of tapiromorph perissodactyls (Mammalia). *Cladistics* **15:** 331–350.

Holbrook LT. 2001. Comparative osteology of early Tertiary tapiromorphs (Mammalia: Perissodactyla). *Zoological Journal of the Linnean Society* **132:** 1–54.

Hoppe KA, Koch PL. 2006. The biogeochemistry of the Aucilla River Fauna. *First Floridians and last Mastodons: the page-ladson site in the Aucilla River*. Netherlands: Springer, 379–401.

Hulbert RC. 1995. The giant tapir, *Tapirus haysii*, from Leisey Shell Pit 1A and other Florida Irvingtonian localities. *Bulletin of the Florida Museum of Natural History* **37:** 515–551.

Hulbert RC. 2005. Late Miocene *Tapirus* (Mammalia: Perissodactyla) from Florida, with description of a new species, *Tapirus webbi*. *Bulletin of the Florida Museum of Natural History* **45:** 465–494.

Hulbert RC. 2010. A new early Pleistocene tapir (Mammalia: Perissodactyla) from Florida, with a review of Blancan tapirs from the state. *Bulletin of the Florida Museum of Natural History* **49:** 67–126.

Hulbert RC, Bloch JI, Poyer AR. 2006. Exceptional preservation of vertebrates from Haile 7G, a new late Pliocene site from Florida. *Journal of Vertebrate Paleontology* **26:** 78A–79A.

Hulbert RC, Wallace SC, Klippel WE, Parmalee PW. 2009. Cranial morphology and systematics of an extraordinary sample of the Late Neogene dwarf tapir, *Tapirus polkensis* (Olsen). *Journal of Paleontology* **83:** 238–262.

Janis CM. 1984. Tapirs as living fossils. In: Eldredge N., Stanley SM, eds. *Casebooks in earth sciences. living fossils*. New York, NY: Springer New York, 80–86.

Klingenberg CP. 2011. MorphoJ: an integrated software package for geometric morphometrics. *Molecular Ecology Resources* **11:** 353–357.

Klingenberg CP. 2016. Size, shape, and form: concepts of allometry in geometric morphometrics. *Development Genes and Evolution* **226:** 113–137.

Koch PL, Hoppe KA, Webb SD. 1998. The isotopic ecology of late Pleistocene mammals in North America. *Chemical Geology* **152:** 119–138.

Kohn MJ, McKay MP, Knight JL. 2005. Dining in the Pleistocene – who's on the menu? *Geology* **22:** 164.

Labonte D, Clemente CJ, Dittrich A, Kuo CY, Crosby AJ, Irschick DJ, Federle W. 2016. Extreme positive allometry of animal adhesive pads and the size limits of adhesion-based climbing. *Proceedings of the National Academy of Sciences of the United States of America* **113:** 1297–302.

MacFadden BJ, Cerling TE. 1996. Mammalian herbivore communities, ancient feeding ecology, and carbon isotopes: a 10 million-year sequence from the Neogene of Florida. *Journal of Vertebrate Paleontology* **16:** 103–115.

MacFadden BJ, Hulbert RC. 1990. Body size estimates and size distribution of ungulate mammals from the Late Miocene Love Bone Bed of Florida. In: Damuth J., MacFadden BJ, eds. *Body size in mammalian paleobiology: estimation and biological implications*. Cambridge: Cambridge University Press, 337–363.

MacLaren JA, Nauwelaerts S. 2016. A three-dimensional morphometric analysis of upper forelimb morphology in the enigmatic tapir (Perissodactyla: Tapirus) hints at subtle variations in locomotor ecology. *Journal of Morphology* **277:** 1469–1485.

MacLaren JA, Nauwelaerts S. 2017. Interspecific variation in the tetradactyl manus of modern tapirs (Perissodactyla: Tapirus) exposed using geometric morphometrics. *Journal of Morphology* **278:** 1517–1535.

van der Made J. 2010. Els macrovertebrats del Camp dels Ninots i el seu context: canvis ambientals, evolució i estructura social. In: Campeny Vall-llosera, G., Gómez de Soler B, eds. *El Camp dels ninots – restres de l'Evolució*. Tarragona: Ayuntament de Caldes de Malavella, Caldes de Malavella & Institut Català de Paleoecologia Humana i Evolució Social, 105–128.

Monteiro LR. 1999. Multivariate regression models and geometric morphometrics: the search for causal factors in the analysis of shape. *Systematic Biology* **48:** 192–199.

Mooney HA, Bullock SH, Ehleringer JR. 1989. Carbon isotope ratios of plants of a tropical dry forest in Mexico. *Functional Ecology* **3:** 137.

Nelson SV. 2014. The paleoecology of early Pleistocene *Gigantopithecus blacki* inferred from isotopic analyses. *American Journal of Physical Anthropology* **155:** 571–578.

Norman JE, Ashley MV. 2000. Phylogenetics of Perissodactyla and tests of the molecular clock. *Journal of Molecular Evolution* **50:** 11–21.

Padilla M, Dowler RC. 1994. *Tapirus terrestris*. *Mammalian Species* **481:** 1–8.

Padilla M, Dowler RC, Downer CC. 2010. *Tapirus pinchaque* (Perissodactyla: Tapiridae). *Mammalian Species* **42:** 166–182.

Perez-Crespo VA, Arroyo-Cabrales J, Alva-Valdivia LM, Morales-Puente P, Cienfuegos-Alvarado E. 2012. Diet and habitat definitions for Mexican glyptodonts from Cedral (San Luis Potosí, México) based on stable isotope analysis. *Geological Magazine* **149:** 153–157.

Qu Y, Jin C, Zhang Y, Hu Y, Shang X, Wang C. 2014. Preservation assessments and carbon and oxygen isotopes analysis of tooth enamel of *Gigantopithecus blacki*

and contemporary animals from Sanhe Cave, Chongzuo, South China during the Early Pleistocene. *Quaternary International* **354:** 52–58.

Radinsky LB. 1965. Evolution of the tapiroid skeleton from *Heptodon* to *Tapirus*. *Bulletin of the Museum of Comparative Zoology* **134:** 69–106.

Revell LJ. 2012. Phytools: an R package for phylogenetic comparative biology (and other things). *Methods in Ecology and Evolution* **3:** 217–223.

Revell LJ. 2013. Two new graphical methods for mapping trait evolution on phylogenies (Freckleton R, ed.). *Methods in Ecology and Evolution* **4:** 754–759.

Rohlf FJ, Slice D. 1990. Extensions of the Procrustes method for the optimal superimposition of landmarks. *Systematic Zoology* **39:** 40–59.

RStudioTeam. 2016. *RStudio: Integrated Development for R*. Boston, MA: RStudio, Inc. Available from: http://www.rstudio.com/.

Ruiz-García M, Vásquez C, Pinedo-Castro M, Sandoval S, Castellanos A, Kaston F, de Thoisy B, Shostell JM. 2012. Phylogeography of the mountain tapir (*Tapirus pinchaque*) and the Central American tapir (*Tapirus bairdii*) and the origins of the three Latin-American tapirs by means of mtCyt-B sequences. In: Anamthawat-Jnsson K, ed. *Current topics in phylogenetics and phylogeography of terrestrial and aquatic systems*. Rijeka: InTechOpen, 83–116.

Ruiz-García M, Castellanos A, Bernal LA, Pinedo-Castro M, Kaston F, Shostell JM. 2016. Mitogenomics of the mountain tapir (*Tapirus pinchaque*, Tapiridae, Perissodactyla, Mammalia) in Colombia and Ecuador: phylogeography and insights into the origin and systematics of the South American tapirs. *Mammalian Biology – Zeitschrift für Säugetierkunde* **81:** 163–175.

Rustioni M, Mazza P. 2001. Taphonomic analysis of *Tapirus arvernensis* remains from the lower valdarno (Tuscany, central Italy). *Geobios* **34:** 469–474.

Schellhorn R, Pfretzschner HU. 2014. Biometric study of ruminant carpal bones and implications for phylogenetic relationships. *Zoomorphology* **133:** 139–149.

Scherler L, Tütken T, Becker D. 2014. Carbon and oxygen stable isotope compositions of late Pleistocene mammal teeth from dolines of Ajoie (Northwestern Switzerland). *Quaternary Research* **82:** 378–387.

Scott KM. 1990. Postcranial dimensions of ungulates as predictors of body size. In: Damuth J., MacFadden BJ, eds. *Body size in mammalian paleobiology: estimation and biological implications*. Cambridge: Cambridge University Press, 301–335.

Secord R, Wing SL, Chew A. 2008. Stable isotopes in early Eocene mammals as indicators of forest canopy structure and resource partitioning. *Paleobiology* **27:** 539–563.

Simpson GG. 1945. Notes on Pleistocene and recent tapirs. *Bulletin of the American Museum of Natural History* **86:** 33–82.

Stacklyn S, Wang Y, Jin C, Wang Y, Sun F, Zhang C, Jiang S, Deng T. 2017. Carbon and oxygen isotopic evidence for diets, environments and niche differentiation of early Pleistocene pandas and associated mammals in South China. *Palaeogeography, Palaeoclimatology, Palaeoecology* **468:** 351–361.

Steiner CC, Ryder OA. 2011. Molecular phylogeny and evolution of the Perissodactyla. *Zoological Journal of the Linnean Society* **163:** 1289–1303.

de Thoisy B, Pukazhenthi B, Janssen DL, Torres IL, May JA Jr, Medici P, Mangini PR, Marquez PAB, Vanstreels RET, Fernandes-Santos RC, Hernandez-Divers S, Quse V. 2014. Tapir Anatomy. *In:* Quse RC, Fernandes-Santos V, eds. *Tapir Veterinary Manual*. Second edition. Campo Grande: IUCN/SSC Tapir Specialist Group.

Tong H. 2005. Dental characters of the Quaternary tapirs in China, their significance in classification and phylogenetic assessment. *Geobios* **38:** 139–150.

Tong H, Qiu ZX. 2008. The perissodactyla. In: Changzhu J, Jinyi L, eds. *Paleolithic site – the Renzidong Cave, Fangchang, Anhui Province*. Beijing: Science Press, 286–320.

Tong H, Liu J, Han L. 2002. On fossil remains of early pleistocene tapir (Perissodactyla, Mammalia) from Fanchang, Anhui. *Chinese Science Bulletin* **47:** 586.

Wiley DF, Amenta N, Alcantara DA, Ghosh D, Kil YJ, Delson, E, Harcourt-Smith W, Rohlf FJ, St. John K, Hamann B, Motani R, Frost S, Rosenberger AL, Tallman L, Disotell T, O'Neill R. 2006. *Landmark editor ver. 3.0*. Davis: Institute for Data Analysis and Visualization (IDAV).

Wood AR, Bebej RM, Manz CL, Begun DL, Gingerich PD. 2011. Postcranial functional morphology of *Hyracotherium* (Equidae, Perissodactyla) and locomotion in the earliest horses. *Journal of Mammalian Evolution* **18:** 1–32.

Zanazzi A, Kohn MJ. 2008. Ecology and physiology of White River mammals based on stable isotope ratios of teeth. *Palaeogeography, Palaeoclimatology, Palaeoecology* **257:** 22–37.

Zelditch ML, Swiderski DL, Sheets HD. 2012. *Geometric morphometrics for biologists: a primer*. New York: Elsevier Academic Press.

SUPPORTING INFORMATION

Additional Supporting Information may be found in the online version of this article at the publisher's web-site:

Appendix S1. List of specimens.

Figure S1. Humeral and radial measurements used to estimate body mass, with graphical representation of body mass calculation for *T. priscus* and *T. arvernensis* (only radius preserved). Measurements correspond to humeral and radial measurements in Scott (1990), equations in MacFadden & Damuth (1990). Bones of *T. pinchaque* (ZMB MAM 62085).

Figure S2. Multivariate regressions of shape variables (Procrustes coordinates) vs. $_{log}$CS from geometric morphometric analysis of 12 forelimb bones of *Tapirus*. A, humerus; B, radius; C, pisiform; D, cuneiform; E, lunate; F, scaphoid; G, magnum; H, unciform; I, MCII; J, MCIII; K, MCIV; L, MCV. Regression score (y-axis) represents combination of shape variables most closely correlated with size variable. Correlation coefficients reported in bottom right of graph.

Table S1. Correlation coefficients from OLS regressions between log-transformed centroid size ($_{log}$CS) and log-transformed body mass ($_{log}$BM), and between the first principal component of shape variables (PC1) of the tapir forelimb and $_{log}$BM (both with ($_{a}R^2$) and without ($_{b}R^2$) extinct taxa). Highest correlations are reported in bold.

Table S2. Results of perMANOVAs of *Tapirus* species, based on regression residuals all forelimb bones corrected for false discovery rate (10 000 permutations). Sum of squares and within-group sum of squares reported alongside *F*-statistic (*F*) and associated *P*-values (*P*). Significant differences in bold.

Table S3. Pairwise comparisons from perMANOVA testing of regression residuals from landmark analysis of *Tapirus* humeri (10 000 permutations). Significant *P*-values (≤0.05) in bold italics.

Table S4. Pairwise comparisons from perMANOVA testing of regression residuals from landmark analysis of *Tapirus* radii (10 000 permutations). Significant *P*-values (≤0.05) in bold italics.

Table S5. Pairwise comparisons from perMANOVA testing of regression residuals from landmark analysis of *Tapirus* pisiforms (10 000 permutations). Significant *P*-values (≤0.05) in bold italics.

Table S6. Pairwise comparisons from perMANOVA testing of regression residuals from landmark analysis of *Tapirus* cuneiform (10 000 permutations). Significant *P*-values (≤0.05) in bold.

Table S7. Pairwise comparisons from perMANOVA testing of regression residuals from landmark analysis of *Tapirus* unciforms (10 000 permutations). Significant *P*-values (≤0.05) in bold.

Table S8. Pairwise comparisons from perMANOVA testing of regression residuals from landmark analysis of *Tapirus* third metacarpals (MCIIIs) (10 000 permutations). Significant *P*-values (≤0.05) in bold.

Table S9. Pairwise comparisons from perMANOVA testing of regression residuals from landmark analysis of *Tapirus* fourth metacarpals (MCIVs) (10 000 permutations). Significant *P*-values (≤0.05) in bold.

Table S10. Pairwise comparisons from perMANOVA testing of regression residuals from landmark analysis of *Tapirus* lunate (10 000 permutations). Significant *P*-values (≤0.05) in bold.

Table S11. Pairwise comparisons from perMANOVA testing of regression residuals from landmark analysis of *Tapirus* scaphoid (10 000 permutations). Significant *P*-values (≤0.05) in bold.

Table S12. Pairwise comparisons from perMANOVA testing of regression residuals from landmark analysis of *Tapirus* magnum (10 000 permutations). Significant *P*-values (≤0.05) in bold.

Table S13. Pairwise comparisons from perMANOVA testing of regression residuals from landmark analysis of *Tapirus* second metacarpal (MCII) (10 000 permutations). Significant *P*-values (≤0.05) in bold.

Table S14. Pairwise comparisons from perMANOVA testing of regression residuals from landmark analysis of *Tapirus* fifth metacarpal (MCV) (10 000 permutations). Significant *P*-values (≤0.05) in bold.

Table S15. Results from phylogenetic signal testing on centroid size (CS) and log centroid size ($_{log}$CS). Performed on species averaged bone data; Pagel's Lambda (λ) and significance of λ statistic (*P*; significant <0.05). Significant *P*-value for λ statistic in bold.

Table S16. One-way analysis of variance (ANOVA) comparing raw stable isotopic values per species, with Tukey's pairwise comparisons. Tukey's Q below pairwise diagonal and *P*-values above the diagonal; significant *P*-values in bold. Abbreviated column titles correspond to species in rows.

Table S17. phyMANOVAs of size-independent shape variables against average stable carbon isotope ($\delta^{13}C$) ranges, based on rPC scores accounting for >70% variance of species averaged shape data (10 000 simulations). Significant values for Wilks' Lambda statistic (Λ) and associated *P*-value (*P*) and phylogenetically corrected *P*-values (corr. *P*) are in bold.

Table S18. phyMANOVAs of size-independent shape variables against average stable carbon isotope ($\delta^{13}C$) ranges, based on the first two rPCs of New World tapir species averaged shape data (10 000 simulations). Cumulative % variance accounted for are presented. Significant values for Wilks' Lambda statistic (Λ) and associated *P*-value (*P*) and phylogenetically corrected *P*-values (corr. *P*) are in bold.